Zero-gap bipolar membrane electrolyzer for carbon dioxide reduction using acid-tolerant molecular electrocatalysts

Bhavin Siritanaratkul,[1] Mark Forster,[1] Francesca Greenwell,[1] Preetam K. Sharma,[2] Eileen H. Yu[2] and Alexander J. Cowan[1]*

1 Stephenson Institute for Renewable Energy and the Department of Chemistry, University of Liverpool, Liverpool, L69 7ZF, UK

2 Department of Chemical Engineering, Loughborough University, Loughborough, LE11 3TU, UK

Supporting Information Placeholder

ABSTRACT: The scaling-up of electrochemical CO_2 reduction requires circumventing the CO_2 loss as carbonates under alkaline conditions. Zero-gap cell configurations with a reverse-bias bipolar membrane (BPM) represent a possible solution, but the catalyst layer in direct contact with the acidic environment of a BPM usually leads to H_2 evolution dominating. Here we show that using acid-tolerant Ni molecular electrocatalysts selective (> 60%) CO_2 reduction can be achieved in a zero-gap BPM device using a pure water and CO_2 feed. At higher current density (100 mA cm^{-2}), CO selectivity decreases, but was still >30%, due to reversible product inhibition. This study demonstrates the importance of developing acid-tolerant catalysts for use in large-scale CO_2 reduction devices.

Electrochemical CO_2 reduction represents a pathway to achieve a circular chemical economy by synthesizing fuels and chemicals from waste CO_2.[1-2] One promising configuration is a zero-gap electrolyzer, with the CO_2 reduction catalyst loaded onto a gas-diffusion electrode (GDE) in direct contact with a cation exchange membrane (CEM), bipolar membrane (BPM), or anion exchange membrane (AEM). Zero-gap structures have been proposed as a route to high current densities and reduced manufacturing costs. Since the catalyst is in close contact with the membrane, the membrane strongly influences the local environment of the catalyst.

The majority of zero-gap studies have utilised AEM's as a high pH limits available protons to achieve selective CO_2 reduction vs H_2 evolution. Whilst this improves selectivity, CO_2 is also 'scavenged' through reaction with hydroxide to form (bi)carbonate, incurring high separation costs.[3] In contrast, BPM and CEM devices, where the catalyst is in contact with the acidic surface of the cation exchange layer, can mitigate this issue, however H_2 formation dominates due to the low pH.[4] Recent work on metal catalysts has shown that selectivity for CO_2 reduction at lower bulk pH can be improved by a high concentration of alkali metal cations[5-7] with liquid electrolyte GDE's and through the use of a polymer buffering layer.[8] Engineering the local pH shows promise, but detrimental carbonate formation within the gas diffusion layer can still occur. An alternative but yet understudied approach is to develop catalysts that are intrinsically selective towards CO_2 reduction in acidic environments.

Few studies have explored the use of molecular catalysts on GDE's for CO_2 reduction, and the majority of these reports have focussed on porphyrin and phthalocyanine complexes of Co and Fe at near neutral or high pH.[9-10] To the best of our knowledge there are no past studies on the use of molecular catalyst modified GDE's in acidic environments. Here we use molecular electrocatalysts with selectivity to CO_2 reduction in acid environments in a zero-gap electrolyzer with a pure-water fed BPM. We used a reverse-biased BPM instead of a simpler CEM system as the sandwiched cation exchange layer/anion exchange layer (CEL/AEL) of the BPM drives water dissociation allowing the anode and cathode to be operated at different pH's. This is beneficial as we achieve the required acidic environment at the cathode and an alkali environment at the anode, which in future studies will allow us to use earth-abundant oxygen evolution catalysts. Furthermore, studies on BPM's in CO_2 reduction have shown low product crossover rates.[11-13] Hydrated CO_2 is flowed at the cathode and deionized H_2O is flowed at the anode. Alkaline solutions are commonly used at the anode due to the lower overpotential for oxygen evolution and higher solution conductivity. However we used pure water which is (i) preferable for scaling up due to low corrosiveness[14-15] and (ii) it avoids the presence of cations (e.g. K$^+$) apart from H$^+$ which will reach the cathode through co-ion transport,[16] changing the local pH and complicating the analysis of the role of the molecular catalyst.

Figure 1 shows the zero-gap cell assembly using a commercial BPM (Fumasep). The molecular catalysts studied here are [Ni(Cyc)]$^{2+}$ (Cyc = cyclam = 1,4,8,11-tetraazacyclotetradecane) and its derivative with a pendant carboxylic acid group [Ni(Cyc-COOH)]$^{2+}$ (CycCOOH = 1,4,8,11-tetraazacyclotetradecane-6-carboxylic acid) which are spray coated onto carbon paper with microporous layers to form the GDE structure (at a loading of 1 mg cm^{-2} with Nafion solution as binder and ion-transporter, for details see SI). [Ni(Cyc)]$^{2+}$ and its derivatives have been studied extensively[17-24] in homogeneous systems and shown to have a high CO selectivity in aqueous systems at pH 2-5, with [Ni(CycCOOH)]$^{2+}$ being particular active at lower pH's.[23, 25] The selectivity at low pH is proposed to be due to high CO_2 binding constant and low pKa of the reduced Ni^I centre.[18-19] There are only two prior reports of Ni cyclam based catalysts immobilized onto a GDE,[26-27] and one with

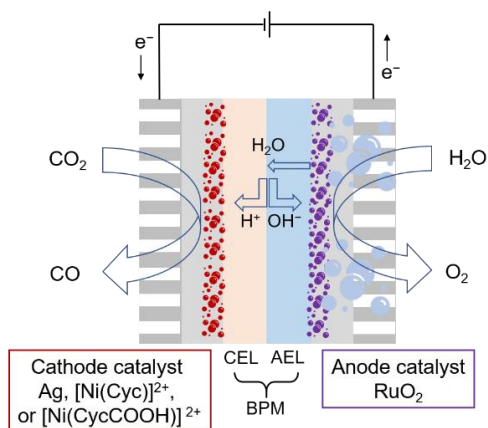the catalyst in a flow cell[25] none of which used an acidic or zero-gap configuration.

Figure 1. *The zero-gap cell with a bipolar membrane*

Figure 2A shows XPS data from the Ni 2p region, with overlapping contributions from F Auger signals (from the PTFE coating on the GDE and Nafion, at 835.0, 862.2, and 882.1 eV). The Ni $2p_{3/2}$ (856.6 eV) and Ni $2p_{1/2}$ (873.8 eV) peaks confirm the presence of $[Ni(Cyc)]^{2+}$ on the GDE. The satellite peaks of Ni $2p_{3/2}$ at 262.3 and 866.2 eV, and Ni $2p_{1/2}$ at 879.4 and 883.8 eV could not be resolved in the $[Ni(Cyc)]^{2+}$ on the GDE surface. Figure 2B-D, S1, and S2 show the Scanning Electron Microscopy (SEM) images and corresponding Ni K_α and F K_α Energy Dispersive X-ray spectroscopy (EDX) elemental mapping of $[Ni(Cyc)]^{2+}$ on a GDE. There were no visible aggregates on the carbon paper substrate and the Ni elemental mapping indicated that the complex was evenly distributed, although smaller aggregates (~1-100 nm scale) cannot be ruled out.
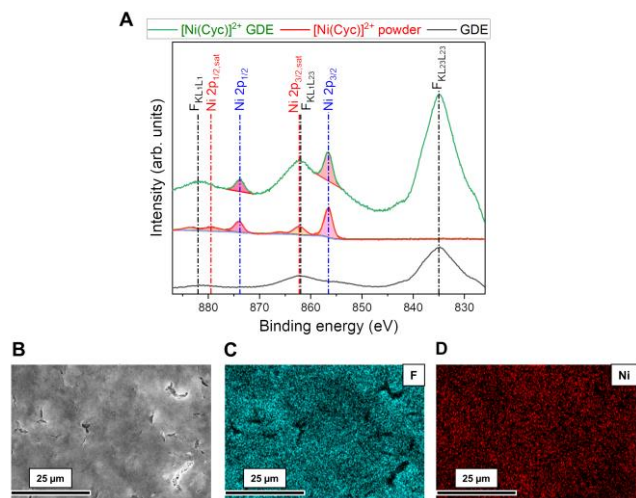

Figure 2. *(A) The XPS Ni 2p spectrum of $[Ni(Cyc)]^{2+}$ on GDE (green), $[Ni(Cyc)]^{2+}$ powder (red), and bare GDE (black). (B) SEM image of $[Ni(Cyc)]^{2+}$ on GDE and corresponding (C) F K_α and (D) Ni K_α EDX maps.*

We conducted chronopotentiometry of the zero-gap cell from 2.5 to 100 mA cm^{-2} for the two molecular catalysts and benchmarked against a commercial Ag nanoparticle catalyst GDE. Ag has been widely studied and is one of the most effective heterogeneous catalyst for CO production.[28-30] The Faradaic efficiency and full cell voltages are shown in Figure 3A, B. When Ag was the

cathode catalyst H_2 was the dominant product at all current densities in-line with past studies of Ag with an acidic electrolyte.[4, 31] The Faradaic efficiency for CO on Ag was very low (10 ± 9 %) at 12.5 mA cm^{-2} and it increased slightly with current density, reaching a maximum of 23 ± 9 % at 50 mA cm^{-2}. The increase in CO selectivity with current density can be explained by the expected increase in the local pH at the electrode surface.[32-34] CO_2 reduction (and H_2 evolution) consumes protons, therefore the proton activity in the boundary layer of the electrolyte is lowered, decreasing H_2 evolution.
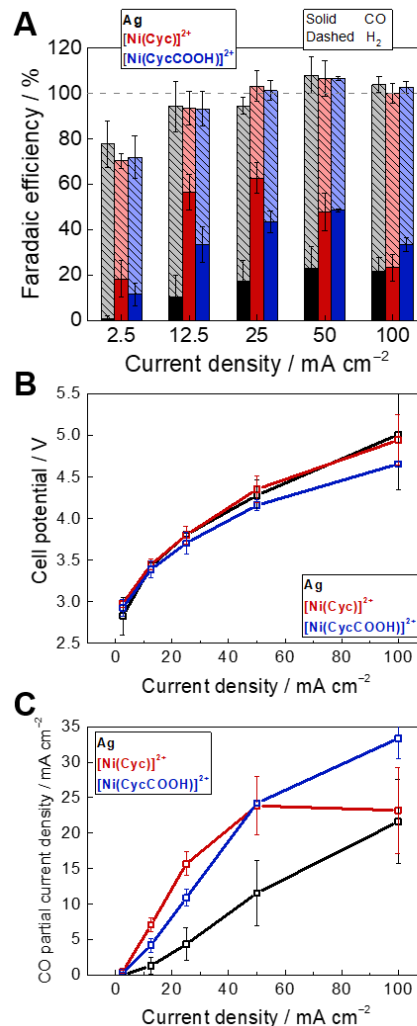

Figure 3. *(A) Initial faradaic efficiency for CO and H_2, (B) full cell potential, and (C) CO partial current density at various total current densities with the cathode catalyst as Ag (black), $[Ni(Cyc)]^{2+}$(red), or $[Ni(CycCOOH)]^{2+}$(blue).*

In contrast the molecular catalysts achieved significantly higher CO Faradaic efficiency across the current range studied here. The maximum CO Faradaic efficiency reached was 63% ± 7 at 25 mA/cm^2 for $[Ni(Cyc)]^{2+}$ and 48% ± 1 at 50 mA/cm^2 for $[Ni(CycCOOH)]^{2+}$. The cell voltages were similar (~2.8 – 5.0 V) across all three cathode catalysts. Although $[Ni(CycCOOH)]^{2+}$ has been reported to achieve higher CO selectivity than $[Ni(Cyc)]^{2+}$ on a Hg electrode in aqueous solution at low pH,[25] in this zero-gap configuration its selectivity was higher only at the highest current density (100 mA cm^{-2}). This may be due to the different nature of the substrate (carbon paper versus Hg). Furthermore, the measured

CO selectivity is the result of complex interplay between the local pH environment, intrinsic CO selectivity, and the sensitivity to CO which was not studied in previous low-current reports.

The performance of molecular catalysts in the acidic environment of our BPM cell is comparable to or exceeds recent results in the literature in which the cathode is in direct contact with the CEL side of the BPM, however in all these cases an elevated local pH has been engineered. Yan et al. used a modified BPM designed to be near neutral (pH ~5) on the CEL side, and reached ~30% CO FE at ~50 mA cm^{-2}.[11] Salvatore et al. investigated the effect of a solid-supported static buffer layer between a Ag cathode and a BPM, and reported a CO FE ~ 10% at 100 mA cm^{-2}, increasing to ~65% with an intermediary buffer layer that would raise the local pH at the cathode.[13]

The CO partial current density (Figure 3C) shows that the activity of the molecular catalysts levelled off, especially for [Ni(Cyc)]$^{2+}$. We estimate a lower limit for the electroactive coverage of [Ni(Cyc)]$^{2+}$ to be $1.5 \pm 0.2 \times 10^{-8}$ mol cm^{-2} through cyclic voltammetry in acetonitrile (Figure S3). Some uncertainty remains due to different solvent penetrations from using acetonitrile, but this coverage of [Ni(Cyc)]$^{2+}$ on a GDE is two orders of magnitude greater than for planar electrodes,[25] however it is only a small fraction of the deposited catalyst (Figure S4) suggesting that future work to obtain higher dispersion of the catalyst could enhance the CO partial current density.

We next considered the possibility of catalyst inhibition by CO formation or catalyst degradation. The change in CO selectivity with time for [Ni(Cyc)]$^{2+}$ is shown in Figure 4A. A constant current measurement at 25 mA cm^{-2} was conducted for 1 h, then the applied current was paused for 1 h with CO_2 and H_2O continuing to flow, then constant 25 mA cm^{-2} was resumed for 1 h. The initial CO selectivity was 71%, which decreased to 31% after operating for 1 h. The CO selectivity recovered after the pause, but decreased again with continued operation. A similar experiment with Ag showed no appreciable change in $CO:H_2$ selectivity with time suggesting that the change is not due to local pH (Figure S5). A test with different wait times on a single sample (Figure 4B) shows that 84% of the initial CO selectivity of [Ni(Cyc)]$^{2+}$ can be recovered after a pause of 15 mins, and the extent of recovery increases with increasing pause duration.

XPS and EDX post electrolysis show substantial loss of Ni from the GDE (Figure S6,7), however, Ni loss as the main deactivation pathway is not consistent with the recovery of selectivity. Instead we consider inhibition of [Ni(Cyc)]$^{2+}$ by the product CO, which can reversibly form an inactive [Ni(Cyc)(CO)]$^{1+}$ species (Figure 4C).[35] In aqueous solution, the CO binding constant of Ni(Cyc)$^{1+}$ is reported to be 4 orders of magnitude higher than its CO_2 binding constant (7.5×10^5 versus 16 M^{-1}).[36-39] Therefore, the inactive [Ni(Cyc)(CO)]$^{1+}$ can accumulate at the CO concentrations (~2-3%) under the highest current density in this study. Another possible concurrent deactivation/recovery pathway is the desorption and re-adsorption of [Ni(Cyc)]$^{2+}$.
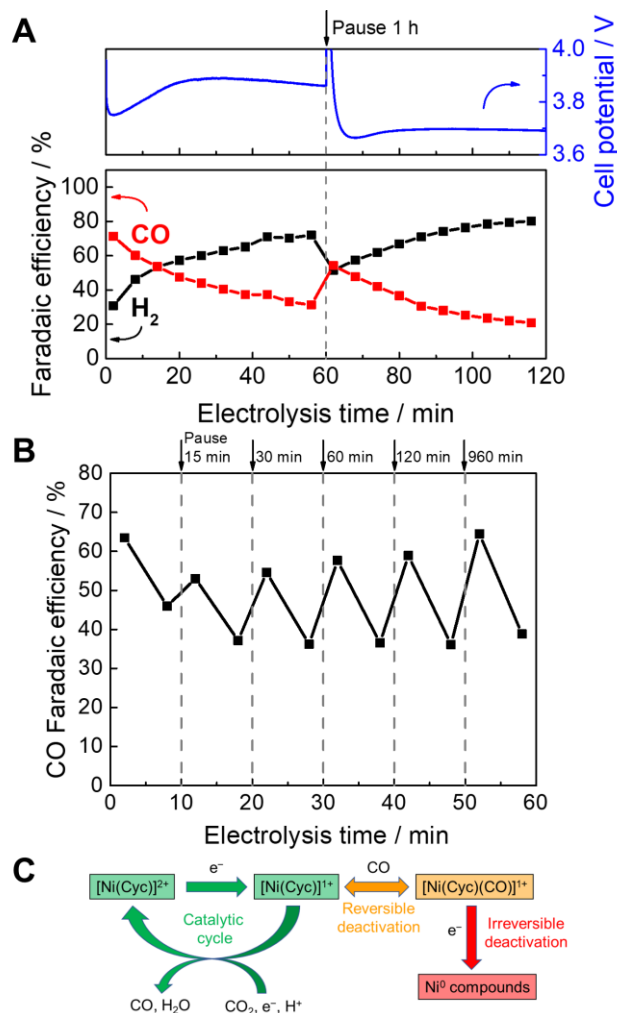

Figure 4. (A) *Operation of [Ni(Cyc)]$^{2+}$ in a BPM zero-gap electrolyzer at a current density of 25 mAcm^{-2} and recovery after a pause. (B) Effect of pausing electrolysis (dashed line) for different time periods on CO FE at 25 mA cm^{-2}. (C) Simplified scheme of CO_2 reduction by [Ni(Cyc)]$^{2+}$ including reversible and irreversible deactivation pathways.*

Since the extent of CO inhibition is proportional to the local CO concentration, the decline in selectivity can be mitigated by optimizing the reaction conditions (Figure 5, S8). In each of these experiments, the measurement was conducted in 30 min segments with a 1 h pause in between each segment to allow the CO-inhibited species to recover. In Figure 5A (conducted in the sequence 20, 40, 80, 10, 20 sccm), the decline in CO FE decreased with increasing CO_2 flow rate, consistent with decreased CO inhibition due to dilution by CO_2. In Figure 5B (conducted in the sequence 25, 12.5, 100, 50, 25 mA cm^{-2}), there was a general trend of faster decline in CO selectivity at higher current density, which would generate more CO. However, the trend is possibly convoluted by a further inactivation process, since a faster rate of deactivation at 25 mA cm^{-2} occurs after going to the highest currents (i.e. most reducing conditions). It is known that under very reducing conditions[40] [Ni(Cyc)(CO)]$^{1+}$ is irreversibly reduced to insoluble Ni^0 compounds.[35] Nevertheless, the results here suggest that at least part of the selectivity limitations can be overcome, for example by optimizing the reaction conditions to avoid irreversible deactivation or by pulsed operation.
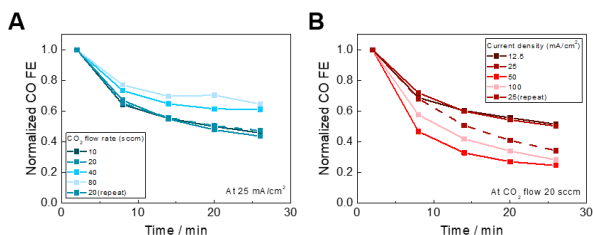
3

Figure 5. *Dependence of CO faradaic efficiency (normalized to the initial point in each segment) by [Ni(Cyc)]$^{2+}$on (A) CO$_2$ flow rate and (B) current density.*

In conclusion, the use of [Ni(Cyc)]$^{2+}$-based molecular catalysts was demonstrated for the first time in a zero-gap CO$_2$ electrolyzer with a BPM, demonstrating improved selectivity for CO$_2$ reduction compared to metallic Ag catalysts up to 100 mA cm^{-2}. This is a rare example of a device using only humidified CO$_2$ and pure water as feedstocks. We also showed the reversible behaviour of CO inhibition, only apparent at high current density, which underscores the importance of catalytic tests under realistic conditions. Our results demonstrate the viability of developing CO$_2$ GDE's that are intrinsically selective in an acidic environment.

ASSOCIATED CONTENT

Supporting Information

Detailed experimental methods, discussion of the source of selectivity at low pH, additional characterization and stability studies. The Supporting Information is available free of charge on the ACS Publications website.

AUTHOR INFORMATION

Corresponding Author

Alexander J. Cowan - Stephenson Institute for Renewable Energy and the Department of Chemistry, University of Liverpool, Liverpool, L69 7ZF, UK; Email: acowan@liverpool.ac.uk

Notes
The authors declare no competing financial interests.

ACKNOWLEDGMENT

REFERENCES

1.   Birdja, Y. Y.; Pérez-Gallent, E.; Figueiredo, M. C.; Göttle, A. J.; Calle-Vallejo, F.; Koper, M. T. M., Advances and challenges in understanding the electrocatalytic conversion of carbon dioxide to fuels. *Nature Energy* **2019,** *4* (9), 732-745.

2.   Kibria, M. G.; Edwards, J. P.; Gabardo, C. M.; Dinh, C.-T.; Seifitokaldani, A.; Sinton, D.; Sargent, E. H., Electrochemical CO$_2$ Reduction into Chemical Feedstocks: From Mechanistic Electrocatalysis Models to System Design. *Adv. Mater.* **2019,** *31* (31), 1807166.

3.   Rabinowitz, J. A.; Kanan, M. W., The future of low-temperature carbon dioxide electrolysis depends on solving one basic problem. *Nature Communications* **2020,** *11* (1), 5231.

4.   Vennekoetter, J.-B.; Sengpiel, R.; Wessling, M., Beyond the catalyst: How electrode and reactor design determine the product spectrum during electrochemical CO2 reduction. *Chem. Eng. J.* **2019,** *364*, 89-101.

5.   Huang Jianan, E.; Li, F.; Ozden, A.; Sedighian Rasouli, A.; García de Arquer, F. P.; Liu, S.; Zhang, S.; Luo, M.; Wang, X.; Lum, Y.; Xu, Y.; Bertens, K.; Miao Rui, K.; Dinh, C.-T.; Sinton, D.; Sargent Edward, H., CO2 electrolysis to multicarbon products in strong acid. *Science* **2021,** *372* (6546), 1074-1078.

6.   Monteiro, M. C. O.; Dattila, F.; Hagedoorn, B.; García-Muelas, R.; López, N.; Koper, M. T. M., Absence of CO2 electroreduction on copper, gold and silver electrodes without metal cations in solution. *Nature Catalysis* **2021,** *4* (8), 654-662.

7.   Monteiro, M. C. O.; Philips, M. F.; Schouten, K. J. P.; Koper, M. T. M., Efficiency and selectivity of CO2 reduction to CO on gold gas diffusion electrodes in acidic media. *Nature Communications* **2021,** *12* (1), 4943.

8.   O'Brien, C. P.; Miao, R. K.; Liu, S.; Xu, Y.; Lee, G.; Robb, A.; Huang, J. E.; Xie, K.; Bertens, K.; Gabardo, C. M.; Edwards, J. P.; Dinh, C.-T.; Sargent, E. H.; Sinton, D., Single Pass CO2 Conversion Exceeding 85% in the Electrosynthesis of Multicarbon Products via Local CO2 Regeneration. *ACS Energy Letters* **2021,** *6* (8), 2952-2959.

9.   Lv, F.; Han, N.; Qiu, Y.; Liu, X.; Luo, J.; Li, Y., Transition metal macrocycles for heterogeneous electrochemical CO2 reduction. *Coord. Chem. Rev.* **2020,** *422*, 213435.

10.   Ren, S.; Joulié, D.; Salvatore, D.; Torbensen, K.; Wang, M.; Robert, M.; Berlinguette, C. P., Molecular electrocatalysts can mediate fast, selective CO<sub>2</sub> reduction in a flow cell. *Science* **2019,** *365* (6451), 367.

11.   Yan, Z.; Hitt, J. L.; Zeng, Z.; Hickner, M. A.; Mallouk, T. E., Improving the efficiency of CO2 electrolysis by using a bipolar membrane with a weak-acid cation exchange layer. *Nature Chemistry* **2021,** *13* (1), 33-40.

12.   Li, Y. C.; Zhou, D.; Yan, Z.; Gonçalves, R. H.; Salvatore, D. A.; Berlinguette, C. P.; Mallouk, T. E., Electrolysis of CO2 to Syngas in Bipolar Membrane-Based Electrochemical Cells. *ACS Energy Letters* **2016,** *1* (6), 1149-1153.

13.   Salvatore, D. A.; Weekes, D. M.; He, J.; Dettelbach, K. E.; Li, Y. C.; Mallouk, T. E.; Berlinguette, C. P., Electrolysis of Gaseous CO2 to CO in a Flow Cell with a Bipolar Membrane. *ACS Energy Letters* **2018,** *3* (1), 149-154.

14.   Lindquist, G. A.; Oener, S. Z.; Krivina, R.; Motz, A. R.; Keane, A.; Capuano, C.; Ayers, K. E.; Boettcher, S. W., Performance and Durability of Pure-Water-Fed Anion Exchange Membrane Electrolyzers Using Baseline Materials and Operation. *ACS Applied Materials & Interfaces* **2021**.

15.   Soni, R.; Miyanishi, S.; Kuroki, H.; Yamaguchi, T., Pure Water Solid Alkaline Water Electrolyzer Using Fully Aromatic and High-Molecular-Weight Poly(fluorene-alt-tetrafluorophenylene)-trimethyl Ammonium Anion Exchange Membranes and Ionomers. *ACS Applied Energy Materials* **2021,** *4* (2), 1053-1058.

16.   Vermaas, D. A.; Wiegman, S.; Nagaki, T.; Smith, W. A., Ion transport mechanisms in bipolar membranes for (photo)electrochemical water splitting. *Sustainable Energy & Fuels* **2018,** *2* (9), 2006-2015.

17.   Beley, M.; Collin, J.-P.; Ruppert, R.; Sauvage, J.-P., Nickel(II)-cyclam: an extremely selective electrocatalyst for reduction of CO2 in water. *J. Chem. Soc., Chem. Commun.* **1984,** (19), 1315-1316.

18.   Beley, M.; Collin, J. P.; Ruppert, R.; Sauvage, J. P., Electrocatalytic reduction of carbon dioxide by nickel cyclam2+ in water: study of the factors affecting the efficiency and the selectivity of the process. *Journal of the American Chemical Society* **1986,** *108* (24), 7461-7467.

19.   Schneider, J.; Jia, H.; Kobiro, K.; Cabelli, D. E.; Muckerman, J. T.; Fujita, E., Nickel(ii) macrocycles: highly efficient electrocatalysts for the selective reduction of CO2 to CO. *Energy & Environmental Science* **2012,** *5* (11), 9502-9510.

20.   Boutin, E.; Merakeb, L.; Ma, B.; Boudy, B.; Wang, M.; Bonin, J.; Anxolabéhère-Mallart, E.; Robert, M., Molecular catalysis of CO2 reduction: recent advances and perspectives in electrochemical and light-driven processes with selected Fe, Ni and Co aza macrocyclic and polypyridine complexes. *Chem. Soc. Rev.* **2020,** *49* (16), 5772-5809.

21.   Jarzębińska, A.; Rowiński, P.; Zawisza, I.; Bilewicz, R.; Siegfried, L.; Kaden, T., Modified electrode surfaces for catalytic reduction of carbon dioxide. *Anal. Chim. Acta* **1999,** *396* (1), 1-12.

22.   Zhanaidarova, A.; Moore, C. E.; Gembicky, M.; Kubiak, C. P., Covalent attachment of [Ni(alkynyl-cyclam)]2+ catalysts to glassy carbon electrodes. *Chem. Commun.* **2018,** *54* (33), 4116-4119.

23.   Neri, G.; Walsh, J. J.; Wilson, C.; Reynal, A.; Lim, J. Y. C.; Li, X.; White, A. J. P.; Long, N. J.; Durrant, J. R.; Cowan, A. J., A functionalised nickel cyclam catalyst for CO2 reduction: electrocatalysis, semiconductor surface immobilisation and light-driven electron transfer. *Physical Chemistry Chemical Physics* **2015,** *17* (3), 1562-1566.

24.   Jiang, C.; Nichols, A. W.; Walzer, J. F.; Machan, C. W., Electrochemical CO2 Reduction in a Continuous Non-Aqueous Flow Cell with [Ni(cyclam)]2+. *Inorg. Chem.* **2020,** *59* (3), 1883-1892.

25.   Neri, G.; Aldous, I. M.; Walsh, J. J.; Hardwick, L. J.; Cowan, A. J., A highly active nickel electrocatalyst shows excellent selectivity for CO2 reduction in acidic media. *Chemical Science* **2016,** *7* (2), 1521-1526.

26.   Pugliese, S.; Huan, N. T.; Forte, J.; Grammatico, D.; Zanna, S.; Su, B.-L.; Li, Y.; Fontecave, M., Functionalization of Carbon Nanotubes with Nickel Cyclam for the Electrochemical Reduction of CO2. *ChemSusChem* **2020,** *13* (23), 6449-6456.

27.   Greenwell, F.; Neri, G.; Piercy, V.; Cowan, A. J., Noncovalent immobilization of a nickel cyclam catalyst on carbon electrodes for CO2 reduction using aqueous electrolyte. *Electrochim. Acta* **2021,** *392*, 139015.

28.   Liu, Z.; Yang, H.; Kutz, R.; Masel, R. I., CO2 Electrolysis to CO and O2 at High Selectivity, Stability and Efficiency Using Sustainion Membranes. *J. Electrochem. Soc.* **2018,** *165* (15), J3371-J3377.

29.   Bhargava, S. S.; Proietto, F.; Azmoodeh, D.; Cofell, E. R.; Henckel, D. A.; Verma, S.; Brooks, C. J.; Gewirth, A. A.; Kenis, P. J. A., System Design Rules for Intensifying the Electrochemical Reduction of CO2 to CO on Ag Nanoparticles. *ChemElectroChem* **2020,** *7* (9), 2001-2011.

30.   Gabardo, C. M.; Seifitokaldani, A.; Edwards, J. P.; Dinh, C.-T.; Burdyny, T.; Kibria, M. G.; O'Brien, C. P.; Sargent, E. H.; Sinton, D., Combined high alkalinity and pressurization enable efficient CO2 electroreduction to CO. *Energy & Environmental Science* **2018,** *11* (9), 2531-2539.

31.   Kim, B.; Ma, S.; Molly Jhong, H.-R.; Kenis, P. J. A., Influence of dilute feed and pH on electrochemical reduction of CO2 to CO on Ag in a continuous flow electrolyzer. *Electrochim. Acta* **2015,** *166*, 271-276.

32.   Gupta, N.; Gattrell, M.; MacDougall, B., Calculation for the cathode surface concentrations in the electrochemical reduction of CO2 in KHCO3 solutions. *J. Appl. Electrochem.* **2006,** *36* (2), 161-172.

33.   Burdyny, T.; Smith, W. A., CO2 reduction on gas-diffusion electrodes and why catalytic performance must be assessed at commercially-relevant conditions. *Energy & Environmental Science* **2019,** *12* (5), 1442-1453.

34.   Bondue, C. J.; Graf, M.; Goyal, A.; Koper, M. T. M., Suppression of Hydrogen Evolution in Acidic Electrolytes by Electrochemical CO2 Reduction. *Journal of the American Chemical Society* **2021,** *143* (1), 279-285.

35.   Balazs, G. B.; Anson, F. C., Effects of CO on the electrocatalytic activity of Ni (cyclam)2+ toward the reduction of CO2. *J. Electroanal. Chem.* **1993,** *361* (1), 149-157.

36.   Schneider, J.; Jia, H.; Muckerman, J. T.; Fujita, E., Thermodynamics and kinetics of CO2, CO, and H+ binding to the metal centre of CO2reductioncatalysts. *Chem. Soc. Rev.* **2012,** *41* (6), 2036-2051.

37.   Fujihira, M.; Hirata, Y.; Suga, K., Electrocatalytic reduction of CO2 by nickel(II) cyclam: Study of the reduction mechanism on mercury by cyclic voltammetry, polarography and electrocapillarity. *Journal of Electroanalytical Chemistry and Interfacial Electrochemistry* **1990,** *292* (1), 199-215.

38.   Fujita, E.; Haff, J.; Sanzenbacher, R.; Elias, H., High Electrocatalytic Activity of RRSS-[NiIIHTIM](ClO4)2 and [NiIIDMC](ClO4)2 for Carbon Dioxide Reduction (HTIM = 2,3,9,10-Tetramethyl-1,4,8,11-tetraazacyclotetradecane, DMC = C-meso-5,12-Dimethyl-1,4,8,11-tetraazacyclotetradecane). *Inorg. Chem.* **1994,** *33* (21), 4627-4628.

39.   Kelly, C. A.; Mulazzani, Q. G.; Venturi, M.; Blinn, E. L.; Rodgers, M. A. J., The Thermodynamics and Kinetics of CO2 and H+ Binding to Ni(cyclam)+ in Aqueous Solution. *Journal of the American Chemical Society* **1995,** *117* (17), 4911-4919.

40.   Froehlich, J. D.; Kubiak, C. P., The Homogeneous Reduction of CO2 by [Ni(cyclam)]+: Increased Catalytic Rates with the Addition of a CO Scavenger. *Journal of the American Chemical Society* **2015,** *137* (10), 3565-3573.

TOC Graphic